3.65-3.71 (m, 4 H), 7.37-7.50 (m, 5 H); CIMS m/z 319 (M + 1). Anal. ($C_{24}H_{38}N_2O_9$) C, H, N.

***N*-[2-[2-(Diethylamino)ethoxy]ethyl]-1-phenyl-1-cyclohexanemethylamine (25).** Compound **25** was prepared (0.23 g, 0.69 mmol, 51%) from **22** (470 mg, 1.36 mmol) according to the procedure described for the synthesis of **24**. The dioxalate hydrate salt was generated by dissolving the free base (0.23 g, 0.69 mmol) in a minimal volume of hot EtOH and adding it to a solution of 0.13 g oxalic acid (1.38 mmol) in hot EtOH. Addition of ether resulted in a white crystalline salt. Recrystallization from EtOH gave the pure oxalate salt of **25**: mp 123-124 °C; ^{1}H NMR (D_2O) δ 1.23 (t, J = 7.3 Hz, 6 H), 1.31-1.72 (m, 8 H), 2.21-2.26 (m, 2 H), 3.12-3.23 (m, 8 H), 3.27 (s, 2 H), 3.65-3.70 (m, 4 H), 7.41-7.57 (m, 5 H); CIMS m/z 333 (M + 1). Anal. ($C_{25}H_{40}N_2O_9 \cdot {}^1/_2H_2O$) C, H, N.

***N*-[2-[2-(Diethylamino)ethoxy]ethyl]-*N*-methyl-1-phenyl-1-cyclopentanemethylamine (26).** A modification of the procedure for N-methylation of amines by Borch and Hassid[18] was used to obtain compound **26**. To a solution of **24** (0.32 g, 1 mmol) in CH_3CN was added 37% formaldehyde (0.24 mL, 3 mmol), followed by $NaBH_3CN$ (0.10 g, 1.6 mmol) at 0 °C. The reaction mixture was allowed to stir at room temperature for 1 h and then was neutralized to pH 6-7 by dropwise addition of glacial acetic acid. After stirring for 45 min, the volatiles were removed in vacuo, and 4 mL of 2 N KOH was added. Extraction with $CHCl_3$ (3 × 100 mL) was followed by washing the combined $CHCl_3$ fractions with 10 mL of 0.5 N KOH, drying, and evaporation of solvent in vacuo to give 0.31 g (92%) of **26** as the crude free base. The dioxalate salt was obtained by dissolving the free base (0.24 g, 0.71 mmol) in a minimal volume of hot MeOH and adding it to a solution of 0.13 g of oxalic acid (1.42 mmol) in MeOH. The solvent was evaporated and the salt was recrystallized from 2-PrOH/ether: mp 107-108 °C; ^{1}H NMR (CD_3OD) δ 1.29 (t, J = 7.2 Hz, 6 H), 1.62-1.68 (m, 2 H), 1.78-1.83 (m, 2 H), 1.90-1.97 (m, 2 H), 2.19-2.27 (m, 2 H), 2.62 (s, 3 H), 3.11-3.21 (m, 4 H), 3.24-3.29 (m, 4 H), 3.64 (s, 2 H), 3.68-3.75 (m, 4 H), 7.28-7.51 (m, 5 H); CIMS m/z 333 (M + 1). Anal. ($C_{25}H_{40}N_2O_9 \cdot {}^1/_2H_2O$) C, H, N.

Anticonvulsant Protocol. Male Sprague-Dawley rats (200-250 g; Zivic-Miller Laboratories), n = 10 per group, were randomly assigned as control of drug-treated animals. Both groups were subjected to a single transauricular maximal electroshock (MES, 2 s at 60 Hz and 50 mA) convulsion delivered through miniature alligator clips attached to the pinna of each ear. All compounds were administered subcutaneously (sc) and tested at 30 min, the time of peak anticonvulsant activity for dextromethorphan.[4] All drugs were freshly prepared using appropriate dilutions in normal saline. Injection volumes were 1-2 mL/kg. Control groups received an appropriate vehicle injection.

Acknowledgment. S.N.C. was supported by a National Research Council Award, sponsored by LTC Marvin Oleshansky, Walter Reed Army Institute of Research. We gratefully acknowledge Dr. Jeffrey Witkin for helpful discussion in preparing this manuscript. We thank Mr. Wesley White for obtaining the NMR spectra and Mr. Noel Whittaker for obtaining the mass spectra. We also thank SSG Lydia Robles and SSG Eddy Echevarria for their technical assistance in running the MES test.

Registry No. **3**, 77-55-4; **4**, 1135-67-7; **5**, 4535-96-0; **6**, 17380-78-8; **7**, 59115-90-1; **8**, 68692-77-3; **9**, 140-82-9; **10**, 79611-69-1; **10**·HCl, 114456-81-4; **11**, 136089-15-1; **11**·oxalate, 136089-25-3; **12**, 136089-16-2; **12**·oxalate, 136115-32-7; **13**, 17380-62-0; **14**, 2890-42-8; **15**, 1074-82-4; **16**, 111-44-4; **17**, 58290-51-0; **18**, 136089-17-3; **19**, 136089-18-4; **20**, 136089-19-5; **20**·2oxalate, 136089-26-4; **21**, 136089-20-8; **21**·fumarate, 136089-27-5; **22**, 136089-21-9; **22**·citrate, 136089-28-6; **23**, 13877-96-8; **23**·citrate, 136089-29-7; **24**, 136089-22-0; **24**·2oxalate, 136089-30-0; **25**, 136089-23-1; **25**·2oxalate, 136089-31-1; **26**, 136089-24-2; **26**·2oxalate, 136089-32-2; 1-phenyl-1-cyclohexanecarbonitrile, 2201-23-2; diethylamine hydrochloride, 660-68-4.

Synthesis, Molecular Modeling Studies, and Muscarinic Receptor Activity of Azaprophen Analogues

David J. Triggle,*,† Yong Who Kwon,† Philip Abraham,‡ J. Bruce Pitner,‡ S. Wayne Mascarella,‡ and F. I. Carroll*,‡

Chemistry and Life Sciences, Research Triangle Institute, Research Triangle Park, North Carolina 27709, and Department of Biochemical Pharmacology, School of Pharmacy, State University of New York at Buffalo, Buffalo, New York 14260.
Received October 29, 1990

Synthesis, radioligand binding, and pharmacologic activities of a series of muscarinic receptor ligands including and related to azaprophen (6-methyl-6-azabicyclo[3.2.1]octan-3α-ol 2,2-diphenylpropionate, **1**) have been measured to determine activity and selectivity for muscarinic receptor subtypes. Pharmacologic affinities of antagonists were determined as pA_2 values for antagonism of methacholine-induced tension responses in guinea pig ileum. Binding affinities were measured by competition against [^{3}H]QNB binding in guinea pig ileum, rat heart and brain, and m_1- or m_3-transfected Chinese hamster ovary (CHO) cells. The efficacies of muscarinic agonists in brain were determined by the ratio of binding affinities against [^{3}H]QNB or [^{3}H]NMS and [^{3}H]oxotremorine-M ([^{3}H]Oxo-M). Nine muscarinic antagonists, including azaprophen, did not discriminate significantly between the subtypes of muscarinic receptors. K_I values for receptor binding for azaprophen (**1**) were between 8.81×10^{-11} and 4.72×10^{-10} M in ileum, heart, brain, and m_1- or m_3-transfected CHO cells. The α- and β-benzilate esters **5** and **6** are as potent as azaprophen, and diphenylacetate esters **3** and **4** and *N*-(6)-benzyl α-isomer **7** are less potent than azaprophen. Significant stereoselectivity was exhibited with (+)-azaprophen being approximately 200 times more potent than the (-)-enantiomers and the 3β-ol isomer **2** being ca. 50 times less potent than azaprophen in all systems. A molecular modeling-molecular mechanics study was conducted to account for the difference. Putative muscarinic agonists (analogues and isomers of 6-methyl-6-azabicyclo[3.2.1]octan-3-ol acetate) did not discriminate muscarinic receptor subtypes with K_I values between 2.77×10^{-6} and 4.33×10^{-5} M without significant stereoselectivity in the systems examined. The most active analogue was (1*R*,3*R*,5*S*)-6-[1(*R*)-phenylethyl]-6-azabicyclo[3.2.1]octan-3α-ol acetate. However, efficacies of these putative agonists were in general very low.

Introduction

A major contributing cause to the cognitive deficit in Alzheimer's disease is a selective degeneration of cholinergic neurons projecting into cortical and hippocampal regions.[1,2] The origin of this deficit is not established, but

† State University of New York at Buffalo.
‡ Research Triangle Institute.

(1) Perry, E. K. The Cholinergic Hypothesis Ten Years On. *Br. Med. Bull.* **1986**, *42* (1), 63-69.
(2) Giacobini, E.; Becker, R. (Eds.) Current Research in Alzheimer Therapy; Taylor and Francis: New York, 1988.

0022-2623/91/1834-3164$02.50/0

Table I. 6-Substituted-6-azabicyclo[3.2.1]octan-3-ol Esters

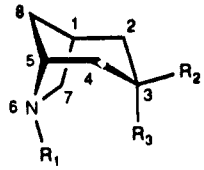

compd	R_1	R_2	R_3	stereochem	method[a]	salt[b]	yield %
1	CH_3	H	$OCOC(CH_3)(C_6H_5)_2$	racemic	A	HCl	31
(+)-1	CH_3	H	$OCOC(CH_3)(C_6H_5)_2$	1*R*,3*R*,5*S*	A	HCl	76
(−)-1	CH_3	H	$OCOC(CH_3)(C_6H_5)_2$	1*S*,3*S*,5*R*	A	HCl	76
2	CH_3	$OCOCCH_3(C_6H_5)_2$	H	racemic	A	HCl	34
3	CH_3	H	$OCOCH(C_6H_5)_2$	racemic	A	$C_4H_4O_4$[d]	28
4	CH_3	$OCOCH(C_6H_5)_2$	H	racemic	A	$C_4H_4O_4$[d]	27
5	CH_3	H	$OCOC(OH)(C_6H_5)_2$	racemic	D	$C_4H_4O_4$[d]	28
6	CH_3	$OCOC(OH)(C_6H_5)_2$	H	racemic	D	$C_4H_4O_4$[d]	6
7	$CH_2C_6H_5$	H	$OCOC(CH_3)(C_6H_5)_2$	racemic	B	HCl	30
8	CH_3	H	$OCOCH_3$	racemic	B	$C_7H_6O_4$[c]	27
(−)-8	CH_3	H	$OCOCH_3$	1*R*,3*R*,5*S*	A	$C_7H_6O_4$[c]	60
(+)-8	CH_3	H	$OCOCH_3$	1*S*,3*S*,5*R*	A	$C_7H_6O_4$[c]	59
9	CH_3	$OCOCH_3$	H	racemic	A	HCl	44
(−)-9	CH_3	$OCOCH_3$	H	1*R*,3*S*,5*S*	C	HCl	66
(+)-9	CH_3	$OCOCH_3$	H	1*S*,3*R*,5*R*	C	HCl	42
10	(*R*)-$CH(CH_3)C_6H_5$	H	$OCOCH_3$	1*R*,3*R*,5*S*	A	HCl	61
11	(*R*)-$CH(CH_3)C_6H_5$	H	$OCOCH_3$	1*S*,3*S*,5*R*	A	HCl	68
12	(*R*)-$CH(CH_3)C_6H_5$	$OCOCH_3$	H	1*R*,3*S*,5*S*	A	HCl	51
13	(*R*)-$CH(CH_30C_6H_5$	$OCOCH_3$	H	1*S*,3*R*,5*R*	A	HCl	50

[a] An example of each procedure is given in the Experimental Section. [b] All compounds except compounds (+)-1, (−)-1, (+)-9, and 11 were recrystallized from a mixture of methanol and ethyl ether. Compounds (+)-9, (+)-1, and 11 were recrystallized from an ethyl acetate and ether mixture and (−)-1 from an ethyl acetate and hexane mixture. [c] Resorcylate. [d] Fumarate.

drugs that increase cholinergic transmission either indirectly by inhibition of acetylcholinesterase or directly by activation of postsynaptic muscarinic receptors are of potential value.[3-5]

Three muscarinic receptors, M_1, M_2, and M_3, have been characterized by selective ligands, and molecular biological studies have revealed the presence of at least five (m_1–m_5) human muscarinic receptor subtypes.[6] It is, however, the pirenzepine-sensitive m_1 receptor, coupled to the stimulation of phosphatidylinositol hydrolysis,[7-9] that is believed to be the most closely linked to the neuronal deficits of Alzheimer's disease. Selective m_1 agonists with appropriate distribution into the brain are, therefore, of potential value. However, clinical experience to date has been disappointing, possibly because the agonists employed, pilocarpine and arecoline, are of low efficacy.[10,11] A search for new effective agonist structures with m_1 selectivity is thus appropriate.

Azaprophen (6-methyl-6-azabicyclo[3.2.1]octan-3α-ol 2,2-diphenylpropionate, 1) was found to be more potent than atropine as an antagonist of peripheral muscarinic responses.[12] The structure of azaprophen suggested that it might interact with the muscarinic receptor in a unique way and could serve as a lead structure for the generation of new and selective muscarinic ligands. Accordingly, a series of analogues of azaprophen has been synthesized and evaluated for their pharmacologic and radioligand binding affinities in smooth muscle, heart, brain, and in m_1 and m_3 muscarinic receptors expressed in Chinese hamster ovary (CHO) cells.[13] This has permitted the comparison of binding and pharmacologic affinities and, for selected compounds, an assessment of their putative agonist efficacies.[11,14]

Results

Synthesis. The 6-substituted-6-azabicyclo[3.2.1]octyl esters shown in Table I were prepared by acylation of the

(3) Moos, W. H.; Davis, R. E.; Schwarz, R. D.; Gamzu, E. R. Cognition Activators. *Med. Res. Rev.* **1988**, *8* (3), 353–369.
(4) Becker, R. E.; Giacobini, E. Mechanisms of Cholinesterase Inhibition in Senile Dementia of the Alzheimer Type: Clinical, Pharmacological, and Therapeutic Aspects. *Drug Dev. Res.* **1988**, *12* (3-4), 163–195.
(5) Wettstein, A.; Speigel, R. Clinical Trials with the Cholinergic Drug R586—Alzheimer's Disease (AD) and Senile Dementia of the Alzheimer Type (SDAT). *Psychopharmacology* **1984**, *84*, 572–573.
(6) Levine, R. R.; Birdsall, N. J. M. (Eds.) Subtypes of Muscarinic Receptors. IV. *Trends Pharmacol. Sci. Suppl.* **1989**, *December*.
(7) Hammer, R.; Berrie, C. P.; Birdsall, N. J. M.; Burgen, A. S. V.; Hulme, E. C. Pirenzepine Distinguishes between Different Subclasses of Muscarinic Receptors. *Nature* **1980**, *283*, 90–92.
(8) Brown, E.; Kendall, D. A.; Nahorski, S. R. Inositol Phospholipid Hydrolysis in Rat Cerebral Cortical Slices: 1. Receptor Characterization. *J. Neurochem.* **1984**, *42* (5), 1379–1387.
(9) Fisher, S. K.; Bartus, R. T. Regional Differences in the Coupling of Muscarinic Receptors to Inositol Phospholipid Hydrolysis in Guinea Pig Brain. *J. Neurochem.* **1985**, *45*, 1085–1095.
(10) Hollander, E.; Mohs, R. C.; Davis, K. L. Cholinergic Approaches to the Treatment of Alzheimer's Disease. *Br. Med. Bull.* **1986**, *42*, 97–100.
(11) Saunders, J.; Cassidy, M.; Freedman, S. B.; Harley, E. A.; Iversen, L. L.; Kneen, C.; MacLeod, A. M.; Merchant, K. J.; Snow, R. J.; Baker, R. Novel Quinuclidine-Based Ligands for the Muscarinic Cholinergic Receptor. *J. Med. Chem.* **1990**, *33*, 1128–1138.
(12) Carroll, F. I.; Abraham, P.; Parham, K.; Griffith, R. C.; Ahmad, A.; Richard, M. M.; Padilla, F. N.; Witkin, J. M.; Chiang, P. C. 6-Methyl-6-azabicyclo[3.2.1]octan-3α-ol 2,2-Diphenylpropionate (Azaprophen), a Highly Potent Antimuscarinic Agent. *J. Med. Chem.* **1987**, *30*, 805–809.
(13) Fraser, C. M.; Wang, C. D.; Robinson, D. A.; Gocayne, J. D.; Venter, J. C. Site-directed Mutagenesis of M_1-muscarinic Acetylcholine Receptors: Conserved Aspartic Acids Play Important Roles in Receptor Function. *Mol. Pharmacol.* **1990**, *36* (6), 840–847.
(14) Freedman, S. B.; Harley, E. A.; Iversen, L. L. Relative Affinities of Drugs Acting at Cholinoceptors in Displacing Agonist and Antagonist Radioligands: the NMS/Oxo-M Ratio as an Index of Efficacy at Cortical Muscarinic Receptors. *Br. J. Pharmacol.* **1988**, *93* (2), 437–445.

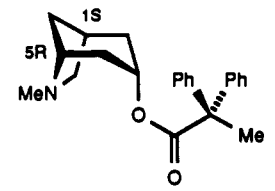

(-)-1
(-) - Azaprophen

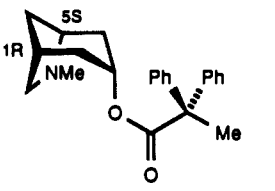

(+)-1
(+) - Azaprophen

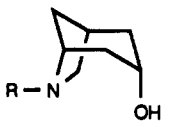

14

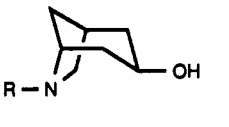

15

a, R = CH_3
b, R = $CH_2C_6H_5$
c, R = $CH(CH_3)C_6H_5$

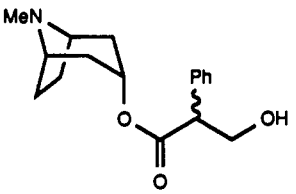

16
Atropine

appropriate azabicyclo alcohol. The physical properties of the esters are listed in Table II. We previously reported that esterification of a mixture of 6-methyl-6-azabicyclo-[3.2.1]octan-3α- and 3β-ols (**14a** and **15a**) with 0.5 equiv of 2,2-diphenylpropionyl chloride in tetrahydrofuran gave 1 plus recovered **15a** hydrochloride.[12] We now report that β-ester **2** was prepared by acylation of a mixture of **14a** and **15a** with excess 2,2-diphenylpropionyl chloride followed by chromatographic separation of **1** and **2**. Acylation of the mixture of **14a** and **15a** with diphenylacetyl chloride or acetyl chloride provided 3α- and 3β-diphenylacetic acid esters **3** and **4** and acetates **8** and **9**, respectively. In each case, the α- and β-isomers were separated by chromatography. 6-Methyl-6-azabicyclo[3.2.1]octan-3β-ol acetate (**9**) was also prepared by treating **15a** hydrochloride with acetyl chloride. Attempts to acylate the mixture of **14a** and **15a** with benzilic acid chloride were unsuccessful. However, esterification with benzilic acid imidazolide provided 3α- and 3β-benzilic esters **5** and **6**, respectively, which were separated by chromatography. Acylation of the mixture of **14b** and **15b** with 2,2-diphenylpropionyl chloride as originally described for the preparation of **1** gave 6-benzyl-6-azabicyclo[3.2.1]octan-3α-ol 2,2-diphenylpropionate (**7**).

The optically active 3α- and 3β-acetates **10** and **11** and **12**, **13**, (+)-**8**, (-)-**8**, (+)-**9** and (-)-**9**, respectively, were prepared by acetylation of the appropriate optically active 6-substituted-6-azabicyclo[3.2.1]octan-3-ol[15] using conditions analogous to those described for the racemic compounds. Esterification of the optically active (+)- and (-)-6-methyl-6-azabicyclo[3.2.1]octan-3α-ol ((+)- and (-)-**14a**) with 2,2-diphenylpropionic acid provided the optically active esters (+)-**1** and (-)-**1**.

Biological Results. Inhibition of Methacholine-Induced Contraction by Muscarinic Antagonists in Guinea Pig Ileum. Methacholine produces biphasic (phasic and tonic) contractile responses in guinea pig ileum. Azaprophen (**1**) and related antagonists dose-dependently inhibited these contractions. Table III lists pA_2 values calculated from Schild analysis and the calculated K_I values. No differences were apparent between the values for the phasic and tonic components of responses consistent with these reflecting different modes of Ca^{2+} mobilization rather than different muscarinic receptor processes.[16] The slopes of the Schild plots were not significantly different from unity consistent with competitive antagonism save for **6**, where the Schild slope was significantly greater than unity.

Competition with [^{3}H]QNB and [^{3}H]Pirenzepine Binding. Table IV summarizes the K_I values and pseudo-Hill coefficients for the azaprophen series of muscarinic antagonists in heart, ileum, brain, and m_1- and m_3-transfected CHO cell membrane preparations against [^{3}H]QNB binding and in brain against [^{3}H]pirenzepine binding. [^{3}H]NMS competition is reported only for atropine, pilocarpine, and carbacol and serves as a standard for comparison. The Hill coefficients are not significantly different from unity, consistent with competitive antagonism. The entire series reveals a fundamental similarity in binding affinities in all systems examined. High stereoselectivity ratios (+/-) of ca. 200 for azaprophen interactions are observed in brain, heart, m_1, and m_3 systems.

Table V summarized the K_I values for a series of putative muscarinic agonists against [^{3}H]QNB binding in heart, brain, and m_1, and m_3 systems. The Hill coefficients are all very close to unity, indicating competitive antagonism.

Competition with [^{3}H]Oxo-M. Table VI summarizes the K_I values of muscarinic agonists against [^{3}H]Oxo-M binding in rat brain and the ratio of affinities against [^{3}H]QNB/[^{3}H]Oxo-M. The values of [^{3}H]QNB/[^{3}H]-Oxo-M and [^{3}H]NMS/[^{3}H]Oxo-M for the control drugs carbachol, pilocarpine, and atropine are included. Control drugs show the same K_I values against [^{3}H]QNB and [^{3}H]NMS, thus we used [^{3}H]QNB/[^{3}H]Oxo-M as an index of efficacy.[11,14] The full agonist carbachol and the antagonist atropine give [^{3}H]QNB/[^{3}H]Oxo-M ratios of ca. 1300 and 1, respectively.

Molecular Modeling

The structures of atropine (**16**), (+)-azaprophen [(+)-**1**], and (-)-azaprophen [(-)-**1**] were compared by molecular modeling methods. The geometric complementarity of the interaction of the active ligands with hypothetical receptor groups was also studied. In general, this involved locating possible sites for the receptor functionality relative to the ligand that would provide for (1) an appropriate range of a receptor carboxylate oxygen atom to the ligand nitrogen atom and (2) no prohibitive steric interactions between the hypothetical receptor functionality and the ring or substituent atoms of active ligands. Goal 1 was satisfied by locating regions where the N-to-O distance would be ca. 2.8 Å while goal 2 was satisfied by monitoring possible differences in steric interaction based on close approaches of ligand and hypothetical receptor group atoms.

Based on X-ray crystallographic data, models of **16** and (+)-**1** (with both endo and exo *N*-methyl groups) were

(15) Pitner, J. B.; Abraham, P.; Joo, Y. J.; Triggle, D. J.; Carroll, F. I. Synthesis and Stereoselective Reduction of (±)-, (+)-, and (-)-6-Substituted-6-azabicyclo[3.2.1]octan-3-one. *J. Chem. Soc., Perkin Trans. 1* **1991**, 1375-1381.

(16) Rosenberger, L. B.; Triggle, D. J. Calcium Ion Utilization in Guinea Pig Ileal Longitudinal Smooth Muscle in Response to a Series of Muscarinic Agonists. *Can. J. Physiol. Pharmacol.* **1979**, *57* (12), 1375-1380.

Table II. Physical Properties of 6-Substituted-6-azabicyclo[3.2.1]octan-3-ol Esters

compd	mp, °C	optical rotation $[\alpha]^{23}_D$ (*c*), deg	formula[a]	^{1}H NMR δ (CH_3OH-d_4) NCH_3	NCHC-$H_3C_6H_5$	COCH_3	C(CH_3)(C_6H_5)$_2$ or CH(C_6H_5)$_2$	CHOCO	others
1	187–191		$C_{23}H_{28}ClNO_2$	2.12			(CH_3) 1.97 (s)	5.35 (t)	7.25 (m, aromatics)
(+)-1	206–208	+6.2 (0.5)	$C_{23}H_{28}ClNO_2$	2.15 (s)			1.97 (s)	5.35 (t)	7.28 (m, aromatics)
(−)-1	206–208	−6.0 (0.5)	$C_{23}H_{28}ClNO_2$	*b*					
2	198–200		$C_{23}H_{28}ClNO_2 \cdot H_2O$	2.88 (s)			(CH_3) 1.87 (s)	5.20 (m)	
3	138–139		$C_{28}H_{29}NO_6$	2.51 (s)			(*H*) 5.12 (s)	5.29 (t)	7.32 (m, aromatics), 6.72 (olefinic)
4	172–175		$C_{28}H_{29}NO_6 \cdot 0.25H_2O$	2.42 (s)			(*H*) 4.96 (s)	5.05 (m)	7.24 (m, aromatics), 6.73 (olefinic)
5	201–202		$C_{24}H_{27}NO_5 \cdot CH_3OH$	2.61 (s)				5.22 (t)	7.37 (m, aromatics), 6.71 (olefinic)
6	178–179		$C_{24}H_{27}NO_5$	2.75 (s)				5.26 (m)	7.37 (m, aromatics), 6.71 (olefinic)
7	230–232		$C_{29}H_{32}ClNO_2$				(CH_3) 2.05 (s)	5.37 (t)	3.82 (d, $CH_2C_6H_5$), 7.34 (m, aromatics)
8	161–162		$C_{17}H_{23}NO_6$	2.07 (s)		2.92 (s)		5.17 (t)	
(−)-8	165–167	−7.8 (0.75)	$C_{17}H_{23}NO_6$	2.01 (s)		2.92 (s)		5.13 (t)	6.61 (t), 6.85 (dd), 7.35 (dd, aromatics)
(+)-8	165.5–167	+8.0 (0.75)	$C_{17}H_{23}NO_6$	*b*					
9	213–214		$C_{10}H_{18}ClNO_2$	2.07 (s)		2.96		5.45 (m)	
(−)-9	217–220	−15.9 (0.98)	$C_{10}H_{18}ClNO_2$	2.02 (s)		2.93 (s)		5.11 (m)	
(+)-9	217–221	+16.2 (1.0)	$C_{10}H_{18}ClNO_2$	*b*					
10	232–235	+19.0 (0.5)	$C_{17}H_{24}ClNO_2$		1.28 (d)	2.10 (s)		5.05 (t)	7.25 (m, aromatics)
11	232–234	+55.6 (0.5)	$C_{17}H_{24}ClNO_2$		1.41 (d)	2.17 (s)		5.07 (t)	7.32 (m, aromatics)
12	234–235	−33.7 (1.0)	$C_{17}H_{24}ClNO_2$		1.29 (d)	2.02 (s)		5.27 (m)	7.32 (m, aromatics)
13	213–214	+44.4 (1.0)	$C_{17}H_{24}ClNO_2$		1.34 (d)	2.01 (s)		5.20 (m)	7.31 (m, aromatics)

[a] All compounds were analyzed for C, H, N; compounds that contained chloride were also analyzed for this element. With the exception of (−)-**9**, the results agreed to within ±0.4% of the theoretical values. The observed C analysis was 0.48% from that calculated. [b] The NMR spectrum was identical to that of its enantiomer. [c] Concentration in MeOH.

Table III. Inhibition of Methacholine-Induced Tension Response in Guinea Pig Ileum by Muscarinic Antagonists

compd	phasic pA_2	phasic slope	phasic −log K_d	tonic pA_2	tonic slope	tonic −log K_d	*n*
1	10.13 ± 0.34	1.23	10.46 ± 0.13	10.38 ± 0.43	1.06	10.39 ± 0.12	12
2	8.73 ± 0.19	0.99	8.44 ± 0.18	8.72 ± 0.16	1.05	8.57 ± 0.19	10
3	8.76 ± 0.23	0.93	8.45 ± 0.15	8.73 ± 0.38	0.94	8.45 ± 0.16	10
4	8.81 ± 0.05	0.87	8.27 ± 0.11	8.74 ± 0.19	0.91	8.32 ± 0.11	10
5	11.19 ± 0.51	1.01	11.11 ± 0.11	11.17 ± 0.73	0.98	10.92 ± 0.12	16
6	8.71 ± 0.03	1.58	9.52 ± 0.22	8.73 ± 0.04	1.58	9.35 ± 0.22	10
7	8.21 ± 0.34	0.86	8.04 ± 0.06	8.25 ± 0.25	0.88	8.03 ± 0.01	17

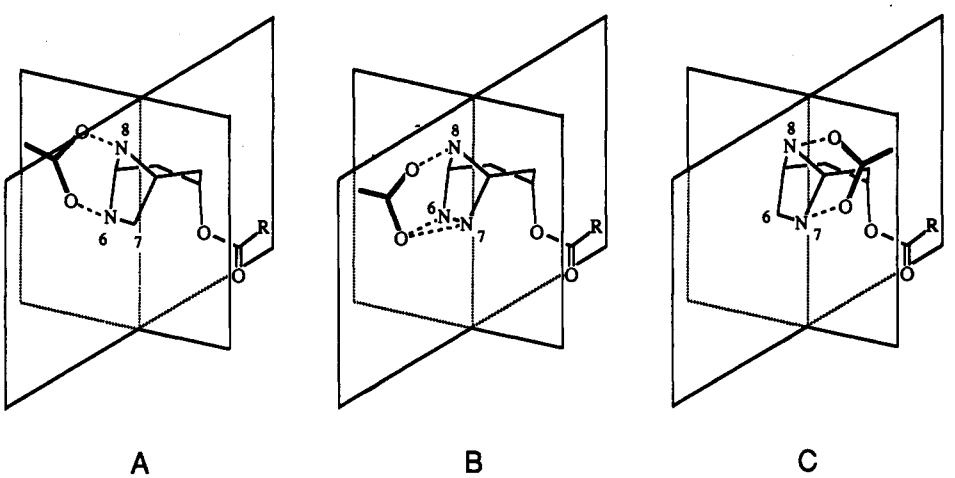

Figure 1. Possible modes of interaction of (+)-azaprophen, (−)-azaprophen, and atropine, with a receptor-site carboxylate group—three limiting cases: case A shows an overlap of (+)-azaprophen and atropine, B an overlay of (+)-azaprophen, (−)-azaprophen, and atropine, and C an overlay of (−)-azaprophen and atropine. (Nitrogen atom positions indicated by atropine ring numbering.)

generated. Each starting structure was then energy-minimized using the SYBYL[17] MAXIMIN2[18] force field (modified to correct the aromatic carbon atom parameters).[19] The structure of (−)-1 was generated by inverting the final structure of (+)-1. The bicyclo[3.2.1]octane ring systems

(17) Tripos Associates, Inc., St. Louis, MO, SYBYL version 5.31.
(18) Clark, M.; Cramer, R. D.; Van Opdenbosh, N. Validation of the General Purpose Tripos 5.2 Force Field. *J. Comput. Chem.* **1989**, *10*, 982–1012.
(19) M. Clark. Tripos Force Field Modification for Aromatic Rings. *SYBYL Update Newsl.* **1990**, *3* (1), 11–12.

Table IV. Inhibition of [^{3}H]QNB and [^{3}H]Pirenzepine Binding by Muscarinic Antagonists

	[^{3}H]QNB																[^{3}H]pirenzepine: brain		
	ileum			heart			brain			m_1			m_3						
compd	K_I	n_H	n	K_I	n_H	n	K_I	n_H	n	K_I	n_H	n	K_I	n_H	n		K_I	n_H	n
1	$2.79 \pm 0.69 \times 10^{-10}$	0.81	8	$1.96 \pm 0.56 \times 10^{-10}$	0.80	6	$1.30 \pm 0.18 \times 10^{-10}$	0.86	6	$8.81 \pm 2.11 \times 10^{-11}$	0.84	9	$4.72 \pm 0.35 \times 10^{-10}$	1.02	6		$1.18 \pm 0.18 \times 10^{-10}$	1.25	4
(+)-1				$5.40 \pm 0.53 \times 10^{-11}$	0.85	4	$2.97 \pm 0.39 \times 10^{-11}$	0.82	4	$3.83 \pm 0.47 \times 10^{-11}$	1.01	4	$9.86 \pm 2.03 \times 10^{-11}$	0.88	4				
(−)-1				$1.45 \pm 0.29 \times 10^{-8}$	1.07	4	$6.36 \pm 1.11 \times 10^{-9}$	0.95	4	$7.89 \pm 2.83 \times 10^{-9}$	1.28	4	$1.07 \pm 0.11 \times 10^{-8}$	1.17	4				
2	$9.64 \pm 1.15 \times 10^{-9}$	0.94	6	$1.29 \pm 0.21 \times 10^{-8}$	0.91	6	$4.20 \pm 0.67 \times 10^{-9}$	0.98	6	$2.94 \pm 0.24 \times 10^{-9}$	1.00	5	$9.28 \pm 1.79 \times 10^{-9}$	1.02	6		$1.27 \pm 0.55 \times 10^{-8}$	0.71	4
3	$8.21 \pm 0.13 \times 10^{-9}$	0.90	6	$5.49 \pm 1.06 \times 10^{-9}$	0.96	6	$1.89 \pm 0.20 \times 10^{-9}$	0.97	6	$1.23 \pm 0.22 \times 10^{-9}$	0.79	7	$4.30 \pm 0.23 \times 10^{-9}$	1.18	6		$2.87 \pm 0.39 \times 10^{-9}$	0.88	4
4	$1.91 \pm 0.13 \times 10^{-8}$	0.92	6	$1.69 \pm 0.12 \times 10^{-8}$	0.94	6	$4.07 \pm 0.72 \times 10^{-9}$	0.85	6	$4.75 \pm 0.62 \times 10^{-9}$	0.91	6	$1.12 \pm 0.14 \times 10^{-8}$	0.96	6		$5.73 \pm 0.94 \times 10^{-9}$	0.94	4
5	$4.49 \pm 0.67 \times 10^{-10}$	0.94	6	$3.02 \pm 0.64 \times 10^{-10}$	0.87	6	$2.54 \pm 0.43 \times 10^{-10}$	0.87	7	$2.20 \pm 0.16 \times 10^{-10}$	0.95	5	$1.12 \pm 0.19 \times 10^{-9}$	0.89	5		$1.97 \pm 0.39 \times 10^{-10}$	1.16	4
6	$4.75 \pm 0.52 \times 10^{-10}$	0.91	6	$2.97 \pm 1.08 \times 10^{-10}$	0.95	6	$2.24 \pm 0.36 \times 10^{-10}$	0.88	6	$1.77 \pm 0.22 \times 10^{-10}$	0.87	8	$6.80 \pm 1.61 \times 10^{-10}$	1.04	6		$1.66 \pm 0.44 \times 10^{-10}$	1.11	4
7	$1.28 \pm 0.18 \times 10^{-8}$	0.94	7	$9.28 \pm 0.16 \times 10^{-9}$	0.89	7	$9.53 \pm 1.00 \times 10^{-9}$	0.83	6	$1.09 \pm 0.20 \times 10^{-8}$	0.83	7	$1.25 \pm 0.28 \times 10^{-8}$	1.09	5		$2.79 \pm 0.98 \times 10^{-9}$	0.83	4

Table V. Inhibition of [^{3}H]QNB and [^{3}H]Pirenzepine Binding by Muscarinic Agonists

	[^{3}H]QNB												[^{3}H]pirenzepine: brain		
	heart			brain			m_1			m_3					
compd	K_I	n_H	n	K_I	n_H	n	K_I	n_H	n	K_I	n_H	n	K_I	n_H	n
8	$8.40 \pm 0.53 \times 10^{-6}$	0.95	4	$7.53 \pm 0.27 \times 10^{-6}$	0.81	6	$9.23 \pm 1.70 \times 10^{-6}$	0.90	8	$8.99 \pm 0.07 \times 10^{-6}$	0.90	6	$9.81 \pm 3.63 \times 10^{-6}$	1.07	4
(+)-8	$2.10 \pm 0.65 \times 10^{-5}$	0.80	7	$8.56 \pm 0.50 \times 10^{-6}$	0.94	7	$1.39 \pm 0.23 \times 10^{-5}$	0.92	4	$1.97 \pm 0.22 \times 10^{-5}$	0.89	4			
(−)-8	$4.19 \pm 0.19 \times 10^{-6}$	0.94	4	$3.73 \pm 0.41 \times 10^{-6}$	0.98	6	$7.21 \pm 0.19 \times 10^{-6}$	1.07	4	$4.97 \pm 0.46 \times 10^{-6}$	0.94	4			
9	$1.19 \pm 0.05 \times 10^{-5}$	1.03	4	$8.55 \pm 0.16 \times 10^{-6}$	1.00	3	$8.62 \pm 2.10 \times 10^{-6}$	0.78	7	$1.41 \pm 0.05 \times 10^{-5}$	0.93	6	$1.25 \pm 0.54 \times 10^{-5}$	0.97	4
(+)-9	$1.04 \pm 0.13 \times 10^{-5}$	0.91	4	$6.47 \pm 0.59 \times 10^{-6}$	1.04	5	$7.11 \pm 1.24 \times 10^{-6}$	0.94	4	$1.13 \pm 0.20 \times 10^{-5}$	0.84	4			
(−)-9	$3.81 \pm 0.29 \times 10^{-5}$	0.85	4	$2.30 \pm 0.38 \times 10^{-5}$	0.97	4	$2.21 \pm 0.20 \times 10^{-5}$	0.98	4	$4.67 \pm 1.39 \times 10^{-5}$	0.81	4			
10	$4.57 \pm 0.33 \times 10^{-6}$	0.78	4	$3.53 \pm 0.25 \times 10^{-6}$	0.90	5	$2.77 \pm 0.28 \times 10^{-6}$	0.74	4	$3.38 \pm 0.76 \times 10^{-6}$	0.76	4			
11	$7.70 \pm 1.33 \times 10^{-6}$	0.98	4	$1.01 \pm 0.10 \times 10^{-5}$	0.90	5	$1.28 \pm 0.19 \times 10^{-5}$	1.02	4	$1.49 \pm 0.38 \times 10^{-5}$	0.89	4			
12	$1.29 \pm 0.07 \times 10^{-5}$	0.81	4	$1.91 \pm 0.12 \times 10^{-5}$	1.00	5	$2.31 \pm 0.29 \times 10^{-5}$	1.03	4	$2.99 \pm 0.88 \times 10^{-5}$	0.91	4			
13	$3.75 \pm 0.23 \times 10^{-6}$	0.90	4	$4.71 \pm 0.30 \times 10^{-6}$	0.98	5	$9.18 \pm 1.11 \times 10^{-6}$	1.05	4	$4.28 \pm 0.38 \times 10^{-6}$	1.03	4			

Table VI. Inhibition of [^{3}H]Oxo-M and [^{3}H]QNB by Muscarinic Agonists in Rat Brain Membranes

	[^{3}H]Oxo-M			[^{3}H]QNB				[^{3}H]NMS			
compd	K_I	n_H	n	K_I	n_H	n	QNB/Oxo	K_I	n_H	n	NMS/Oxo
atropine	$4.59 \pm 1.65 \times 10^{-10}$	0.92	3	$3.37 \pm 0.48 \times 10^{-10}$	1.00	4	0.73	$3.00 \pm 0.37 \times 10^{-10}$	0.97	4	0.65
carbachol	$1.31 \pm 0.16 \times 10^{-8}$	1.11	4	$1.88 \pm 0.32 \times 10^{-5}$	0.56	4	1435.11	$1.88 \pm 0.39 \times 10^{-5}$	0.66	4	1435.11
pilocarpine	$8.29 \pm 3.35 \times 10^{-8}$	0.95	4	$1.01 \pm 0.16 \times 10^{-6}$	0.95	5	12.18	$1.11 \pm 0.02 \times 10^{-6}$	0.86	4	13.39
8	$1.15 \pm 0.06 \times 10^{-6}$	1.04	4	$7.53 \pm 0.03 \times 10^{-6}$	0.87	3	6.55				
(+)-8	$2.17 \pm 0.20 \times 10^{-6}$	0.93	4	$8.56 \pm 0.50 \times 10^{-6}$	0.94	7	3.94				
(−)-8	$6.55 \pm 0.28 \times 10^{-7}$	1.10	4	$3.73 \pm 0.41 \times 10^{-6}$	0.98	6	5.69				
9	$7.82 \pm 0.25 \times 10^{-6}$	1.01	4	$8.55 \pm 0.02 \times 10^{-6}$	1.00	3	1.09				
(+)-9	$1.04 \pm 0.13 \times 10^{-5}$	1.24	4	$6.47 \pm 0.59 \times 10^{-6}$	1.04	5	0.62				
(−)-9	$3.39 \pm 0.13 \times 10^{-6}$	0.96	4	$2.30 \pm 0.38 \times 10^{-5}$	0.97	4	6.78				
10	$1.13 \pm 0.09 \times 10^{-7}$	1.05	4	$3.53 \pm 0.25 \times 10^{-6}$	0.90	5	31.24				
11	$1.95 \pm 0.25 \times 10^{-6}$	0.86	4	$1.01 \pm 0.10 \times 10^{-5}$	0.90	5	5.18				
12	$2.33 \pm 0.25 \times 10^{-5}$	0.65	4	$1.91 \pm 0.12 \times 10^{-5}$	1.00	5	0.82				
13	$4.15 \pm 0.28 \times 10^{-6}$	0.76	4	$4.71 \pm 0.30 \times 10^{-6}$	0.98	5	1.13				

of all structures were then overlayed using the SYBYL command FIT. Using an Evans & Sutherland PS-330 workstation, a generalized carboxylate group was manually docked to the overlayed model structures while monitoring the distance between the two carboxylate oxygens and each of the ring nitrogens of **16**, (+)-1, and (−)-1. Sites around the overlayed substrates were sought that would allow for nitrogen-to-oxygen distances of ca. 2.8 Å between either carboxylate oxygen and one nitrogen atom from *both* **16** and either (+)-1 or (−)-1. As illustrated in Figure 1, three general locations for the carboxylate satisfying the above conditions were identified by this method. With the carboxylate group aligned along the long axis of the ring system (case B), the carboxylate oxygen atoms can be brought into ca. 2.8-Å range of nitrogen atoms located at positions 6, 7, or 8 (atropine numbering) on the ring. The carboxylate group in this case lies in a longitudinal plane that bisects the bicyclo[3.2.1]octan-3α-ol ring. Alternatively, positioning the carboxylate to either side of the ring affords 2.8 Å N-to-O distances between the carboxylate and nitrogen atoms at positions 8 and 6 (case A) *or* 8 and 7 (case C). The carboxylate group in these two cases lies in a lateral plane orthogonal to the longitudinal plane described above.

In order to provide an estimate of the differences between endo and exo *N*-methyl conformers in steric interaction between the hypothetical receptor carboxylate group and the *N*-methyl group, the distance between the closest carboxylate oxygen atom and the *N*-methyl carbon atom was evaluated for each conformer. For atropine/case A, this difference in C-to-O distance was found to be 0.056 Å, and in case B the difference was 1.85 Å. Azaprophen/case A yielded an endo/exo difference in C-to-O distance of 0.045 Å and in case B a difference of 1.002 Å.

Discussion

A comparison of the pA_2 values listed in Table III shows that azaprophen (1) and the corresponding benzilate ester **5** were the most potent in the antagonist series with the other compounds being 10–100-fold less active. The binding affinities given in Table IV show that azaprophen (1) and α- and β-benzilate esters **5** and **6** were the most potent in all systems examined, with **1** being slightly more active than **5** and **6** in all systems. Comparison of the data also shows that none of the nine antagonists, including azaprophen, discriminated significantly between the subtypes. However, a general trend for the compounds to be some 5-fold less active in the m_3 system compared to the m_1 system was noted.

The 200-fold stereoselectivity observed for (+)-1 over (−)-1 in brain, heart, m_1, and m_3 systems is the most significant finding from these studies. Two imortant questions are raised by the relative activities of atropine[12] and (+)- and (−)-azaprophen: (1) why are the 6-aza [(+)-azaprophen] and 8-aza (atropine) compounds both more active than the 7-aza [(−)-azaprophen] compound and (2) given the apparent degree of freedom in locating the nitrogen atom noted above, why does moving the nitrogen to the 7-position ((−)-azaprophen) cause a 200-fold loss of activity?

Three-dimensional molecular modeling demonstrates that the geometry of the interaction between a hypothetical binding-site carboxylate group and azabicyclic ligands can account for the selective activity of 6- and 8-azabicyclo[3.2.1]octan-3-ols. As illustrated schematically in Figure 2, if the ester side chain of the ligand is anchored by an interaction with a hydrophobic receptor pocket (L1) and a hydrogen-bond interaction involving the ester carbonyl oxygen and a receptor hydrogen-bond donor site

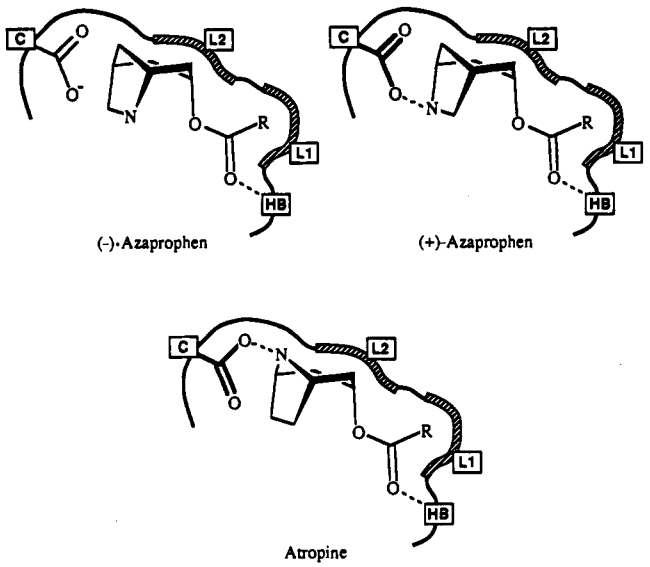

Figure 2. Schematic representation of the association of (+)-azaprophen, (−)-azaprophen, and atropine with the postulated muscarinic receptor site carboxylate group (C), lipophilic pockets (L1 and L2), and the hydrogen bonding group (HB).

(HB) and the cationic head group associates with an anionic receptor site disposed to one side of the ring system (as specified in Figure 1, case A), then either atropine or (+)-azaprophen would be expected to bind well to the receptor. (Note that this three-point pharmacophore model (C, L1, HB) does not exclude the possibility of other lipophilic interactions with the bicyclic ring methylenes (L2).) The involvement of a carboxylate residue in binding to the muscarinic receptor has been inferred by several workers from studies of the strong homologies in the sequence data available on muscarinic, adrenergic, dopamine, and serotonin receptors.[6] It has been noted in a previous report[12] that a carboxylate is a particularly appropriate anionic functional group as it would provide a bidentate coordination site for optimal association with either a 6-aza- or 8-azabicyclo[3.2.1]octanol. In the case of (−)-azaprophen, however, the position of the nitrogen relative to the ester side chain would not permit association with the proposed hydrogen-bonding, hydrophobic, and anionic sites.

It is interesting to note that based on this pharmacophore, characterized by a lateral carboxylate group (Figure 1, case A), the contribution to binding efficiency provided by the carboxylate/nitrogen atom interaction should be relatively insensitive to the conformation of the *N*-methyl group. This conclusion is suggested by the *N*-methyl carbon atom to carboxylate oxygen atom distances determined by molecular modeling. In case A for both atropine and azaprophen, the differences for this close approach are relatively small (<0.1 Å). (In contrast, in case B the endo/exo C-to-O distance differences are >1 Å for both ligands.)

The six analogues, including two stereoisomeric pairs, of 6-methyl-6-azabicyclo[3.2.1]octan-3-ol did not discriminate muscarinic receptor subtypes as shown by the binding data in Table V. In addition, no significant stereoselectivity was observed with the enantiomeric pairs (+)- and (−)-**8** and (+)- and (−)-**9**. Examination of the [^{3}H]QNB/[^{3}H]Oxo-M data in Table VI indicates low ratios for all the acetates with the highest being for (1*R*,3*R*,5*S*)-6-[(*R*)-phenylethyl]-6-azabicyclo[3.2.1]octan-3α-ol acetate (**10**). Compounds (−)-**8**, (−)-**9**, **10**, and **11** showed values similar to those for the weak partial agonist pilocarpine and the other agents have ratios of ~1. Pre-

vious work of others[11,14] suggests that these ratios for (−)-8, (−)-9, 10, and 11 may indicate agonists of low efficacy or, where ratios are apparently unity, antagonists.

Conclusion

The synthesis, radioligand binding, and pharmacologic activities of a series of muscarinic ligands derived from 6-substituted-6-azabicyclo[3.2.1]octan-3-ol have provided new information concerning the muscarinic antagonist and agonist pharmacophore. The conclusions are (a) this azabicyclo ring system shows significant enantioselectivity as well as stereoselectivity with 1*R*,3*R*,5*S* isomer (+)-azaprophen being 200 times more potent than 1*S*,3*S*,5*R* isomer (−)-azaprophen and β-esters **2**, **4**, **5** being less active than their α-analogues **1**, **3**, and **6**; (b) none of the antagonist analogues of this ring system, including azaprophen, discriminated significantly between the subtypes of muscarinic receptors; (c) antagonists as potent as azaprophen can be obtained by changing the ester group (see benzylate ester **5**); (d) none of the putative muscarinic agonists thus far evaluated discriminate muscarinic receptor subtypes; and (e) the most potent putative agonist **10** has the same absolute stereochemistry as the most potent antagonist (+)-**1**.

Experimental Section

Synthesis. Melting points were determined on a Thomas Hoover capillary tube apparatus. All optical rotations were determined at the sodium D line using a Rudolph Research Autopol III polarimeter (1-dm cell). NMR spectra were recorded on a Bruker WM-250 spectrometer using tetramethylsilane as an internal standard. High-resolution mass spectra were obtained on a VG Analytical ZAB E spectrometer. Thin-layer chromatography was carried out on Whatman silica gel 60 TLC plates using $CHCl_3$/MeOH/concentrated NH_4OH (40:9:1) unless otherwise noted. Visualization was accomplished under UV or in an iodine chamber. For column chromatography, a 230–400 mesh silica gel and a $CHCl_3$/MeOH/concentrated NH_4OH (40:9:1) mixture was used as eluent. Microanalyses were carried out by Atlantic Microlab, Inc.

6-Substituted-6-azabicyclo[3.2.1]octan-3-ol Esters. Method A. The appropriate amino alcohol in CH_2Cl_2 (6 mL/mmol) at 0 °C was treated successively with triethylamine (1.25 equiv), 4-(dimethylamino)pyridine (0.1 equiv), and the appropriate acid chloride or acetic anhydride (1.5 equiv) under N_2 and was stirred for 18 h at room temperature. The mixture was neutralized with 20% NH_4OH at 0 °C. The aqueous phase was extracted three times with CH_2Cl_2. The combined organic fractions were dried over Na_2SO_4. The residue obtained on evaporation of the solvent under reduced pressure was purified by column chromatography on SiO_2.

Method B. To a stirred solution of a mixture of the 3α- and 3β-isomers of 6-substituted-6-azabicyclo[3.2.1]octan-3-ol (2 equiv) in dry THF (5 mL/mmol) at 0 °C was added the appropriate acid chloride (1 equiv) in dry THF (5 mL/mmol), and stirring was continued for 18 h at room temperature. The precipitate was removed by filtration. The residue obtained on evaporation of the filtrate was purified by silica gel column chromatography.

Method C. The corresponding *N*-α-methylbenzyl esters were treated with Pd/C (10 mol%) and ammonium formate (3 equiv) in MeOH (10 mL/mmol) and gently heated to reflux for 3 h. The catalyst was removed by filtration. The solvent was evaporated under reduced pressure. The residue was taken up in CH_2Cl_2 and was washed with saturated NaCl solution. The dried solution (Na_2SO_4) was evaporated to dryness under reduced pressure. The residue in methanol (10 mL/mmol) along with Pd/C and paraformaldehyde (3 equiv) was hydrogenated under atmospheric pressure for 4 h. The catalyst was filtered off, and the residue was evaporated to dryness and purified on silica gel.

Method D. An equimolar mixture of isomeric amino alcohols and benzilic acid imidazolide (prepared from equivalent amounts of benzilic acid and carbonyldiimidazole) in acetone (10 mL/mmol of alcohol) was heated to reflux for 3 h. The solvent was removed under reduced pressure, and the isomeric esters were separated by silica gel column chromatography.

Molecular Modeling. Molecular modeling was performed using the SYBYL software package,[17] running on Digital Equipment Corporation microVAX II's and VAXstation 3110 workstations. An Evans & Sutherland PS 330 graphics workstation and a Macintosh IIcx interfaced to the VAX cluster were used for display and real-time manipulation of three-dimensional molecular models.

In order to generate starting structures, the X-ray crystallographic coordinates of atropine (**16**) and azaprophen (**1**) were input using the CRYSIN command. The structures were energy-minimized with the MAXIMIN2 force field. A model of (−)-azaprophen was then obtained by inverting the minimized structure of (+)-azaprophen. The final structures of atropine and (+)- and (−)-azaprophen were overlayed using the SYBYL root-mean-square FIT command. All the corresponding pairs of non-hydrogen ring atoms of each structure were superimposed.

The two orthogonal planes bisecting the bicyclo[3.2.1]octan-3α-ol ring systems were defined using atoms 8 and 3 and the C-3 oxygen (longitudinal plane) and atoms 6–8 (lateral plane). A generalized carboxylate group (essentially an acetate anion) was constructed using molecular fragments contained in the SYBYL software package. The manual docking of the carboxylate with the superimposed ligand molecules was performed using the MONITOR command to probe the various nitrogen-to-oxygen distances.

Biological Tissue Preparation and Recording of Response. Guinea pig ileal longitudinal smooth muscle was employed to measure an in vitro pharmacologic potency of muscarinic agents. In brief, male Albino guinea pigs (Buckberg Farms, Tomkins Cove, NY, weighing 300–500 g) were killed by decapitation, and the terminal ileum was dissected.[19] Longitudinal muscle strips (1–2 cm) were mounted in 10-mL organ baths containing physiologic salt solution of the following composition (millimolar): NaCl, 118.4; KCl, 4.7; $CaCl_2$, 1.9; $NaHCO_3$, 25; $MgSO_4$, 1.2; KH_2PO_4; glucose, 11.7, maintained at 37 °C and aerated with 95% O_2:5% CO_2. Tissues were equilibrated for 45 min under a resting tension of 500 mg with the bathing medium being changed every 15 min. A cumulative dose–response curve was then constructed to methacholine and the tissue washed. When the tension had returned to resting level, the tissues were allowed to equilibrate for 15 min before incubating for 45 min with antagonist, followed by the construction of a second cumulative dose–response curve to methacholine. To allow for any change in sensitivity between the two curves, controls were performed with tissues not exposed to the antagonist. All responses were measured isometrically using Grass-FT03 force-displacement transducer and recorded on Grass Polygraph (Model 7D).

Cell Cultures. Transfected CHO cell lines specifically expressing rat m_1 or m_3 muscarinic receptor subtypes were employed.[13] Cells were cultured in monolayers in 100-mm plastic tissue culture dishes in medium-containing 90% nutrient mixture F-M (Ham's), 10% fetal bovine serum, 2 mM L-glutamine, 50 units/mL penicillin, and 50 μg/mL streptomycin in a humidified atmosphere of 95% O_2:5% CO_2. Geneticin (50 μg/mL) was added to the medium to prevent the loss of cell lines expressing cloned receptor genes. Cells were subcultured at a density of $3–5 \times 10^4$ cells per mL of medium, and cultures became confluent by day 3 with a density of $2–5 \times 10^5$ cells per dish containing 10 mL of medium.

Preparation of Tissues and Cell Cultures for Radioligand Binding. Microsomal fractions of guinea pig ileum, rat heart, and rat brain were prepared as described previously in our laboratory.[20–22] In brief, male albino guinea pigs and male

(20) Bolger, G. T.; Gengo, R.; Klockowski, R.; Luchowski, E.; Siegel, H.; Janis, R. A.; Triggle, A. M.; Triggle, D. J. Characterization of Binding of the Ca^{2+} Channel Antagonist, [^{3}H]Nitrendipine, to Guinea-Pig Ileal Smooth Muscle. *J. Pharmacol. Exp. Ther.* **1983**, *225*, 291–310.

(21) Janis, R. A.; Sarmiento, J. G.; Maurer, S. C.; Bolger, G. T.; Triggle, D. J. Characteristics of the Binding of [^{3}H]Nitrendipine to Rabbit Ventricular Membranes: Modification by Other Ca^{++} Channel Antagonists and by the Ca^{++} Channel Agonist Bay K 8644. *J. Pharmacol. Exp. Ther.* **1984**, *231*, 8–15.

Sprague–Dawley rats were killed by decapitation. The longitudinal smooth muscle and rat brain minus cerebellum and brain stem were minced with scissors in 15 vol/g wet wt in ice-cold 50 mM Tris buffer (pH 7.2, 25 °C) with 10 passes of motor-driven (TRI-R-Stirrer) glass–Teflon homogenizer at setting 7. Rat heart homogenate was prepared in a similar fashion, save that it was first homogenized in a Brinkman Polytron at setting 7 for 5 s.[21] The CHO cells expressing m_1 or m_3 receptors were suspended in 50 mM ice-cold tris buffer and homogenized with a motor-driven glass–Teflon homogenizer at setting 5 with 10 passes. The ileal, brain, heart, and m_1 and m_3 muscarinic receptor expressing cell line homogenates were centrifuged at 1100*g* for 20 min, and the supernatants were recentrifuged at 45000*g* for 45 min at 4 °C. The resultant pellet was resuspended in ice-cold 50 mM Tris buffer at a concentration of 10–20, 20–30, 120–150, 5–8, and 10–15 μg per 5-mL binding assay volume for ileum, brain, heart, and m_1 and m_3 expressing cell line preparations, respectively, for the QNB binding assay. For the pirenzepine binding assay, 50–80 μg of brain protein per 1-mL binding assay volume was used. For [^{3}H]Oxo-M binding, the rat brain membrane pellet was prepared in the same way in 20 mM HEPES buffer (pH 7.4), the pellet was washed once and centrifuged at 45000*g* for 45 min, and the resultant pellet was resuspended at a concentration of 30–40 μg per 1-mL assay volume. Protein concentrations were measured by the method of Bradford[23] with bovine serum albumin as standard.

[^{3}H]QNB, [^{3}H]Pirenzepine, [^{3}H]Oxo-M, and [^{3}H]NMS Radioligand Binding. The method described by Jim et al.[22] was employed. Membrane fractions were incubated with 4.56×10^{-11} M [^{3}H]QNB and various concentrations of muscarinic agents in a 5-mL binding assay volume at 25 °C for 60 min for tissue preparations, for 90 min for m_1 receptor expressing cell membranes, and for 120 min for m_3 receptor expressing cell membrane fractions. In brain membranes, 2.44×10^{-9} M [^{3}H]pirenzepine, 1.15×10^{-9} M [^{3}H]Oxo-M or 5.08×10^{-11} M [^{3}H]NMS was incubated with muscarinic agents in 1-mL binding assay volume for 60 min for [^{3}H]pirenzepine and [^{3}H]Oxo-M and in a 5-mL volume for 90 min for [^{3}H]NMS. These incubating times were determined in control experiments to be adequate for equilibration to be achieved. Radioligand concentrations employed were determined from separate saturation experiments to be lower than the K_D values. After incubation, samples were filtered over Whatman GF/B filters and washed twice with 5 mL of ice-cold Tris buffer using a cell harvester (Model M-24R, Brandel Instrument, Gaithersberg, MD). For [^{3}H]Oxo-M experiments, samples were filtered over GF/C filters presoaked in 0.05% polyethylenimine. The radioactivity of filters in 5 mL of scintillation fluid was counted using liquid scintillation counter at an efficiency of approximately 45%. Nonspecific binding was measured in the presence of 10^{-5} M atropine.

Materials. [^{3}H]QNB (L-[*Benzilic*-4,4′-^{3}H]-quinuclidinyl benzilate, specific activity 43.9 Ci/mmol), [^{3}H]pirenzepine ([*N-methyl*-^{3}H]-pirenzepine, specific activity 87.1 Ci/mmol), [^{3}H]-Oxo-M ([*methyl*-^{3}H]-oxotremorine-M acetate, specific activity 87.0 Ci/mmol), and [^{3}H]NMS ([*N-methyl*-^{3}H]-scopolamine methyl chloride, specific activity 78.9 Ci/mmol) were purchased from Du Pont-New England Nuclear (Boston, MA). Tissue culture media and supplements were obtained from GIBCO Laboratories (Grand Island, NY).

Data Analysis. Pharmacologic data were calculated as percent of maximum response and EC_{50} values calculated by probit analysis. pA_2 values were calculated by Schild plots, and K_D values were calculated from the equation $-\log K_D = (\log DR - 1) - \log [B]$. Radioligand binding data were analyzed using a nonlinear curve fitting program (BDATA, CDATA, EMF Software, Knoxville, TN) implemented on an IBM personal computer. K_D values were calculated by the method of Cheng and Prusoff.[24]

Acknowledgment. This research was supported by Grant AG-07418 from the National Institute on Aging.

(22) Jim, K.; Bolger, G. T.; Triggle, D. J.; Lambrecht, G. A Study of Muscarinic Receptors by Agonist [^{3}H]-Labeled Antagonist Competition. *Can. J. Physiol. Pharmacol.* **1982**, *60*, 1707–1714.

(23) Bradford, M. M. A Rapid and Sensitive Method for the Quantitation of Microgram Quantities of Protein Utilizing the Principle of Protein-dye Binding. *Anal. Biochem.* **1976**, *72*, 248–253.

(24) Cheng, Y. E.; Prisoff, W. H. Relations between the Inhibition Constant (K_I) and the Concentration of an Inhibitor that Causes a 50% Inhibition (I_{50}) of an Enzymatic Reaction. *Biochem. Pharmacol.* **1973**, *22*, 3099–3108.